Model-Based Intelligent Fault Detection and Diagnosis for Mating Electric Connectors in Robotic Wiring Harness Assembly Systems

Jian Huang, *Member, IEEE*, Toshio Fukuda, *Fellow, IEEE*, and Takayuki Matsuno, *Member, IEEE*

***Abstract*—Mating a pair of electric connectors is one of the most important steps in a robotic wiring harness assembly system. A class of piecewise linear force models is proposed to describe both the successful and the faulty mating processes of connectors via an elaborate analysis of forces during different phases. The corresponding parameter estimation method of this model is also presented by adapting regular least-square estimation methods. A hierarchical fuzzy pattern matching multidensity classifier is proposed to realize fault detection and diagnosis for the mating process. This classifier shows good performance in diagnosis. A typical type of connectors is investigated in this paper. The results can easily be extended to other types. The effectiveness of proposed methods is finally confirmed through experiments.**

***Index Terms*—Fault detection and diagnosis, fuzzy pattern matching, modeling, robotic wiring harness assembly.**

I. Introduction

AUTOMATED handling of assembly of materials has been studied by many researchers in the areas of manufacturing, robotics, and artificial intelligence. While robotic assembly applications have increased in both number and complexity over the years, a large number of applications have been passed over due to technology. One of them is the electric wiring harness assembly task, which presents itself in the manufacturing of various electrical instruments. To implement a robotic wiring harness assembly system as shown in Fig. 1, researchers have to tackle two primary issues. One is using robotic systems to manipulate deformable linear objects (DLOs), which has been extensively discussed in [1] and [2]. The other is how to obtain a secured mating of a pair of electric connectors by the assembly robot. However, so far, little work has been done with respect to this issue.

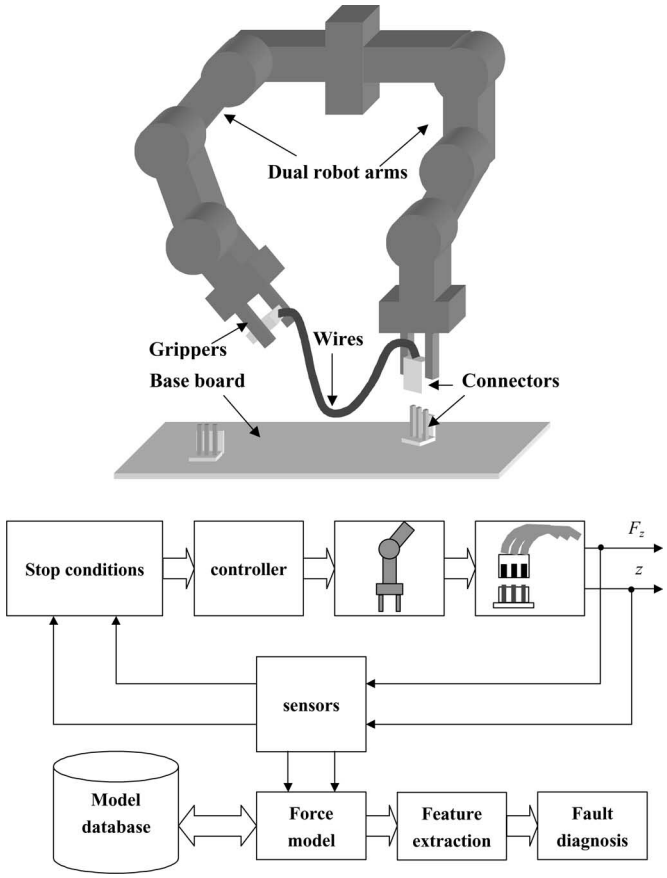

Fig. 1. Concept of a robotic wiring harness assembly system and the scheme of model-based FDD for the mating process.

In a robotic assembly system, error recovery approaches are necessary due to inevitable errors caused by unpredictable situations. The field of error recovery is often divided into three subfields: *fault detection*, *diagnosis*, and *error recovery* [3]. During the last decades, many efforts have been made in the field of fault detection and diagnosis (FDD), especially in the field of model-based methods [4]–[8]. On the other hand, intelligent methods, like neural networks (NNs) or neuro-fuzzy approaches, are also extensively applied to FDD systems. However, these methods always treat systems as "black-box" models, in which the *a priori* knowledge is overlooked.

For a fault diagnosis problem, statistical methods are usually not good choices because they require large numbers of training samples to estimate probability distributions. Therefore, intelligent classifiers, especially fuzzy classifiers, are widely applied

Manuscript received August 12, 2007; revised December 20, 2007. Recommended by Guest Editors F. Karray and C.W. de Silva. This work was supported in part by the New Energy and Industrial Technology Development Organization (NEDO) as a part of "Project for Strategic Development of Advanced Robotics Elemental Technologies". The work of J. Huang was supported by the National Natural Science Foundation of China under Grant 60603006.

J. Huang is with the Department of Micro-Nano Systems Engineering, Nagoya University, Nagoya 464-8603, Japan. He is also with the Department of Control Science and Engineering, Huazhong University of Science and Technology, Hubei 430074, China (e-mail: huang@robo.mein.nagoya-u.ac.jp).

T. Fukuda is with the Department of Micro-Nano Systems Engineering, Nagoya University, Nagoya 464-8603, Japan (e-mail: fukuda@mein.nagoyau.ac.jp).

T. Matsuno is with the Department of Intelligent System Design Engineering, Toyama Prefectural University, Imizu City 939-0398, Japan (e-mail: matsuno@pu-toyama.ac.jp).

Digital Object Identifier 10.1109/TMECH.2007.915063

in this field. Real-time performance of some fuzzy classification methods has been evaluated in [9]. Among them, the fuzzy pattern matching (FPM) method seems to be the best one since it gives very good classification rates for the shortest computing time and it possesses the incremental learning ability [10]. Although the traditional FPM method cannot classify nonconvex shapes, recently some improvements have been proposed to solve the problem [11]. A hierarchical diagnosis scheme, called SELECT, has been presented and applied to dc motors [12]. A hierarchical fuzzy pattern matching classifier (HFPMC), which combined the FPM method and a decision tree, was successfully applied in [13] to recognize tire treads.

In this paper, a model-based fault detection and diagnosis scheme for the mating process of electric connectors is investigated. For each type of connector, a typical frictional force model is established to describe the whole mating process. All the typical models are integrated into a database in advance. During a mating process, the impedance and the displacement of the gripper are measured by sensors mounted in the robot. Both force and displacement limits are preset as stop conditions. If either of the stop conditions is satisfied, model parameters are estimated as features from the sensor data, which serve to the feature extraction and fault diagnosis modules. A hierarchical fuzzy pattern-matching scheme (HFPMS) is chosen as the final classifier.

II. Modeling for the Mating Process of Connectors

A. Introduction to Electric Connectors

In view of the variety of electric connectors that we may meet in different tasks, it is necessary to establish a model database that comprises all possible cases. Despite the fact that the characteristics of connectors differ from each other, their underlying frictional force models are similar during a mating process. Therefore, instead of enumerating all possible cases, we investigate a special type of connectors to exemplify the modeling procedure. Applying similar methods to other types, a model database as depicted in Fig. 1 can finally be constructed. The typical connectors and headers studied in this paper are illustrated in Fig. 2. As we can see, there are a couple of lead-in chamfers on the connector and the header, respectively. These chamfers provide a positive locking that provides a secure mating retention.

The aforementioned "*force model*" means the relationship of resistance F_z that impedes connector's insertion, and the corresponding displacement z of the gripper. Both these signals are measured by sensors mounted in the robot. It should be pointed out that such a model is not a dynamic model describing the plant states, because the model parameters exclude input forces from the robot.

B. Modeling for Successful Mating Process

In order to model the mating process, it is necessary to analyze the process of insertion carefully and to separate force data into components from different sources. A typical mating process of the insertion can be divided into four phases, which are shown in Fig. 2.

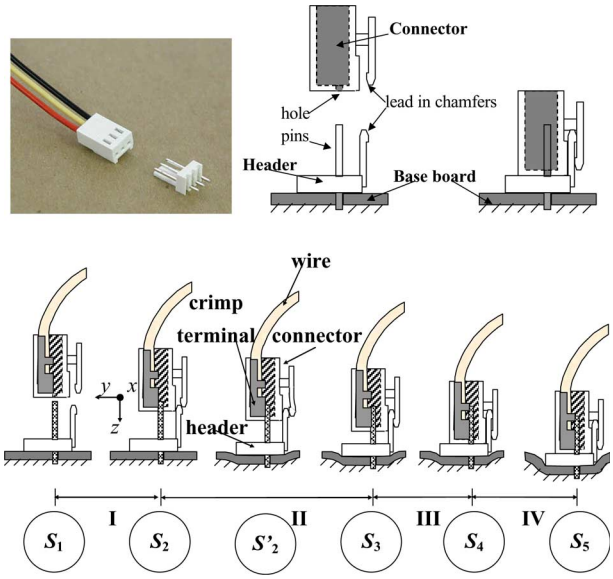

Fig. 2. Pair of typical three-pin connector and header, and their typical mating process with four key phases.

During all these phases, a female socket connector prewired with standard wires, which are clamped tightly together with crimp terminals, is mated with the header little by little. We use $\{S_i, S_{i+1}\}$ to denote the start and end state of a phase, where $i = 1, 2, \ldots, 4$. S_2' is an intermediate state in phase II. The definition of reference frame is also shown in Fig. 2.

1) Phase I: The connector starts to move down from a state at which it is totally separated from the header to a state at which it slightly touches the header. Note that, at the end of this phase, the couple of lead-in chamfers comes into contact and are ready to lead the connector to slide in. During this phase, the z-axis resistance F_z is approximately equal to zero.

2) Phase II: A detailed force analysis of this phase is depicted in Fig. 3. The z-axis force F_z mainly comes from two sliding frictions, $F_{\mathrm{fr}1}$ and $F_{\mathrm{fr}2}$. During the insertion, deformations occur in several places, including pins, crimp terminals, chamfers, and even the base board. Some deformations produce increasing normal forces upon frictional surfaces, which makes the force F_z become larger as the connector wedges in deeper. We based our consideration on the following assumptions.

Assumption 1: The two frictions satisfy $F_{\mathrm{fr}1} \gg F_{\mathrm{fr}2}$, since the contact surface between two lead-in chamfers is very smooth. This assumption leads to

$$F_z = F_{\mathrm{fr}1}. \tag{1}$$

Assumption 2: Suppose that all the deformations are elastic. These consist of deformations of crimp terminals and pins, and the deformation of the two lead-in chamfers. Obviously, the extent of the deformations depends on the depth of the insertion. Therefore, in phase II, we can suppose that the normal forces on the contact surface and their counterparts F_1, F_2, F_1', F_2', which are produced by these deformations, are proportional to the relative displacement increment between the connector and

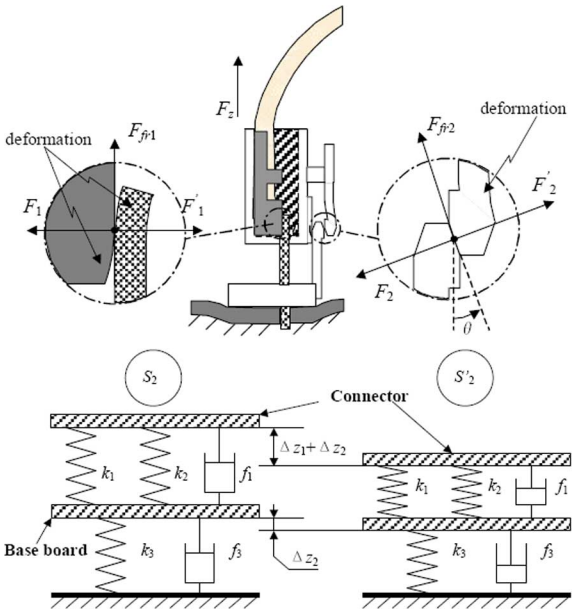

Fig. 3. Force analysis and mechanical system model of phase II.

the header. Thus, we have

$$F_1 = k'_1\,\Delta z_1, \qquad F_2 = k'_2\,\Delta z_1 \tag{2}$$

where Δz_1 denotes the relative displacement increment, and k'_1 and k'_2 are the proportional parameters.

Assumption 3: In view of the fact that the gripper's speed is slow and constant in the whole mating process, we assume a simple friction model without considering the variance of frictions due to different speed. That is to say, the frictions satisfy

$$\begin{aligned} F_{\mathrm{fr1}} &= \mu_1 \cdot (F_1 + F_2\,\cos\,\theta) + f_1 \\ &= k_1\,\Delta z_1 + k_2\,\Delta z_1 + f_1 \end{aligned} \tag{3}$$

where μ_1 is the fictional parameter determined by the Coulomb's friction law, k_1 and k_2 are elastic constants, and f_1 is the static friction.

Assumption 4: A single-point contact model is introduced to describe the deformation of the base board. In spite of the small measurement, this deformation always exists during the mating, caused by the pressure F_z coming from the header. This model is parameterized by k_3 and f_3 in Fig. 3.

Together with the single-point contact model, we can formulate a corresponding mechanical system model shown in Fig. 3 for phase II. In this mechanical system, the upper two springs describe the two friction components derived from normal forces F_1 and F_2. These two components are quantified as two items in (3). The parameter Δz_2 indicates the deformation of the base board. The parameter $\Delta z_1 + \Delta z_2$ is the actual relative z-axis displacement increment of the connector. Introduce $z_{\mathrm{I,II}}$, $z_{\mathrm{II,III}}$, and $z_{\mathrm{III,IV}}$ to denote the displacements of the boundary states, S_2, S_3, and S_4, between every two successive phases. In the reference frame defined in Fig. 2, the

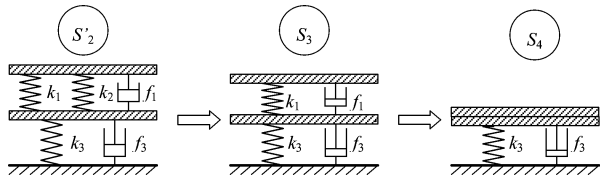

Fig. 4. Transitions of the mechanical system models.

equations

$$F_z = k_3\,\Delta z_2 + f_3 \tag{4}$$

$$\Delta z = \Delta z_1 + \Delta z_2 = z - z_{\mathrm{I,II}} \tag{5}$$

hold. Equations (1)–(5) can be summed up to a concise force model of phase II, which is given by

$$F_z = k_{\mathrm{II}} z + f_{\mathrm{II}} \tag{6}$$

where parameters k_{II} and f_{II} satisfy

$$\begin{cases} k_{\mathrm{II}} = \dfrac{k_3(k_1+k_2)}{k_1+k_2+k_3} \\ f_{\mathrm{II}} = \dfrac{k_3 f_1 + (k_1+k_2) f_3}{k_1+k_2+k_3} - k_{\mathrm{II}} z_{\mathrm{I,II}}. \end{cases} \tag{7}$$

3) Phase III: The frictional component produced by two lead-in chamfers disappears suddenly when entering state S_3 because the slippage between chamfers is over. Thus, a transition of corresponding mechanical system models happens, which is depicted in Fig. 4.

Applying a similar procedure as in phase II, the force model of phase III is easily obtained as follows:

$$F_z = k_{\mathrm{III}} z + f_{\mathrm{III}} \tag{8}$$

where

$$k_{\mathrm{III}} = \frac{k_1 k_3}{k_1+k_3}, \qquad f_{\mathrm{III}} = \frac{k_3 f_1 + k_1 f_3}{k_1+k_3} - k_{\mathrm{III}} z_{\mathrm{I,II}}. \tag{9}$$

4) Phase IV: After the connector and the header are totally mated, friction forces between them disappear immediately. Therefore, the system model is changed again. Such a transition is also depicted in Fig. 4.

The mathematical expression of the force model in phase IV is then easily obtained as follows:

$$F_z = k_{\mathrm{IV}} z + f_{\mathrm{IV}} \tag{10}$$

where

$$k_{\mathrm{IV}} = k_3, \quad f_{\mathrm{IV}} = f_3 - k_{\mathrm{IV}} z_{\mathrm{I,II}}. \tag{11}$$

5) Boundary Analysis: The boundaries are those displacements $z_{\mathrm{I,II}}$, $z_{\mathrm{II,III}}$, $z_{\mathrm{III,IV}}$ at which a transition of the force model occurs. Except for $z_{\mathrm{I,II}}$, sudden changes of F_z occur before and after the boundaries, because some of the force components disappear just after the transition of models. The changes of F_z at all the boundaries are denoted by $\Delta F_{\mathrm{I,II}}$, $\Delta F_{\mathrm{II,III}}$, and $\Delta F_{\mathrm{III,IV}}$.

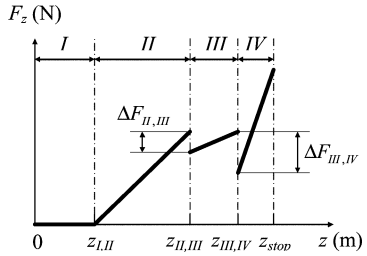

Fig. 5. Typical force profile of a successful mating process.

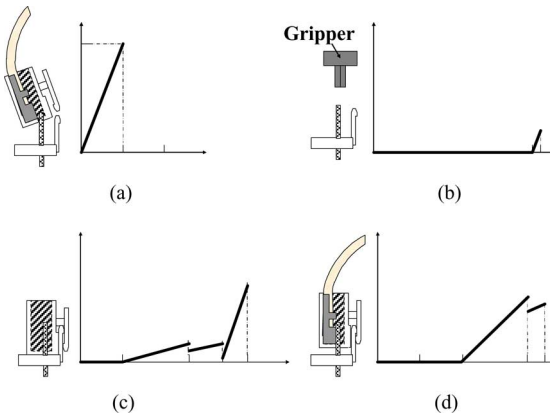

Fig. 6. Models for four classes of fault mating processes. (a) Jammed insertion. (b) Connector lost. (c) Wrong connector. (d) Uncompleted insertion.

To sum up the aforementioned analyses for all phases, we conclude a piecewise linear model to describe the whole mating process as

$$F_z = \begin{cases} 0, & 0 \le z \le z_{\mathrm{I,II}} \\ k_{\mathrm{II}} z + f_{\mathrm{II}}, & z_{\mathrm{I,II}} < z \le z_{\mathrm{II,III}} \\ k_{\mathrm{III}} z + f_{\mathrm{III}}, & z_{\mathrm{II,III}} < z \le z_{\mathrm{III,IV}} \\ k_{\mathrm{IV}} z + f_{\mathrm{IV}}, & z_{\mathrm{III,IV}} < z \end{cases} \tag{12}$$

where all the parameters are given by (7), (9), and (11). Note that the relation among three slope parameters is $k_{\mathrm{III}} < k_{\mathrm{II}} < k_{\mathrm{IV}}$. In addition, the boundary positions are found uncertain from observing the experiment results. Fuzzy tools are used to cope with these uncertainties, as illustrated in Section II-D. A typical profile of the complete force model can then be shown by Fig. 5. The validation of the model is discussed in Section V.

C. Modeling for Fault Cases

In this study, four common fault cases often met in the mating process are modeled by using the similar methods presented in Section II-B. These faults include *jammed insertion*, *connector lost*, *wrong connector*, and *uncompleted mating*. Note that wrong connectors here indicate connectors wrongly prewired with improper number of wires. The schematic drawings and the ideal force profiles are given in Fig. 6. It should be pointed out that the parameters and boundaries in fault cases are also uncertain.

As shown in Fig. 6, similar piecewise linear models can be developed for possible faults. The analytical representations of these models are concluded in Table I. To avoid the confusion of notations, we use a superscript i to indicate different fault classes with $i = 0, 1, \ldots, 4$, where value 0 stands for the successful case.

D. Parameter Estimation

Least-square estimation (LSE) is a well-known tool to estimate coefficients of a straight line. Unfortunately, it cannot be directly applied to our piecewise linear model due to the uncertainties of boundaries. Commonly, these uncertainties can be solved by assigning some fuzzy sets to characterize different phases of the mating process. Reference fuzzy sets of each phase are obtained based on the experimental data and designers' experience. To determine the optimal degree of overlaps and shapes of the fuzzy membership functions is a tough task. Whereas, we have also experienced that a rough choice will often give satisfying results. For a linguistic variable set {PHASE I, PHASE II, PHASE III, PHASE IV}, the corresponding membership functions are displayed in Fig. 7. A set of commonplace trapezoid functions $\{\mu_{\mathrm{I}}(z), \mu_{\mathrm{II}}(z), \mu_{\mathrm{III}}(z), \mu_{\mathrm{IV}}(z)\}$ are assumed to characterize these fuzzy sets.

For the whole process, a piecewise linear approximator is formulized as

$$\hat{F}_z(z) = \sum_{i=I}^{\mathrm{IV}} \mu_i(z)(\hat{k}_i z + \hat{f}_i) \tag{13}$$

where $\hat{F}_z$ denotes the estimated z-axis force for the given displacement z. The coefficients $\hat{k}_i$ and $\hat{f}_i$ are estimated parameters of the linear models. The membership functions $\mu_i(z)$ are used as weighting factors that define the different segments $i \in \{\mathrm{I}, \mathrm{II}, \mathrm{III}, \mathrm{IV}\}$. Given a set of n training samples $T = \{(z_k, F_{z,k})\}$, the parameters of the linear models can be trained. The goal is to minimize the approximation errors for the training samples that are located in one phase. On the other hand, training samples that belong to another phase could have arbitrary bad approximation results. These parameters are typically determined by the regular LSE method by minimizing the LSE function

$$J = \sum_{k=1}^{n} (F_{z,k} - \hat{F}_z(z_k))^2 \tag{14}$$

over the training set.

Note that the idea of an approximator (13) is similar to those presented in [14] and [15], in which a class of Gaussian functions are adopted as the weighting factors.

III. Extracting Features for Fault Diagnosis

In this paper, we regard implementing our FDD system as a multiclasses classification task based on a feature space composed of all possible estimated model parameters.

Feature extraction is the process of transforming the raw data into a format that both highlights the class differences in the

TABLE I
IDEAL PIECEWISE LINEAR MODELS FOR SUCCESSFUL MATING AND FAULT CASES

Success ($i = 0$)	Jammed Insertion ($i = 1$)	Connector Lost ($i = 2$)
$F_z = \begin{cases} 0, & 0 \le z \le z_{I,II}^{(0)}, \\ k_{II}^{(0)} z + f_{II}^{(0)}, & z_{I,II}^{(0)} < z \le z_{II,III}^{(0)}, \\ k_{III}^{(0)} z + f_{III}^{(0)}, & z_{II,III}^{(0)} < z \le z_{III,IV}^{(0)}, \\ k_{IV}^{(0)} z + f_{IV}^{(0)}, & z_{III,IV}^{(0)} < z. \end{cases}$	$F_z = k_I^{(1)} z + f_I^{(1)}$	$F_z = \begin{cases} 0 & 0 \le z \le z_{I,II}^{(2)}, \\ k_{II}^{(2)} z + f_{II}^{(2)}, & z_{I,II}^{(2)} < z. \end{cases}$

Uncompleted Insertion ($i = 3$)	Wrong Connector ($i = 4$)
$F_z = \begin{cases} 0, & 0 \le z \le z_{I,II}^{(3)}, \\ k_{II}^{(3)} z + f_{II}^{(3)}, & z_{I,II}^{(3)} < z \le z_{II,III}^{(3)}, \\ k_{III}^{(3)} z + f_{III}^{(3)}, & z_{II,III}^{(3)} < z. \end{cases}$	$F_z = \begin{cases} 0, & 0 \le z \le z_{I,II}^{(4)}, \\ k_{II}^{(4)} z + f_{II}^{(4)}, & z_{I,II}^{(4)} < z \le z_{II,III}^{(4)}, \\ k_{III}^{(4)} z + f_{III}^{(4)}, & z_{II,III}^{(4)} < z \le z_{III,IV}^{(4)}, \\ k_{IV}^{(4)} z + f_{IV}^{(4)}, & z_{III,IV}^{(4)} < z. \end{cases}$

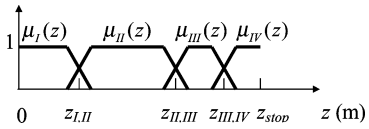

Fig. 7. Fuzzy segmentation for the phases of a successful mating process.

data and converts it to a form that can be compatible with the classifier. Owing to the *a priori* knowledge of force models, the most useful features must be the parameters in the complete models. These parameters include the coefficients k and f of every linear segment and the *standard square errors* derived from the procedure of parameter estimation. A feature space can be established based on all these parameters, whose dimension depends on both the number of fault cases and the complexity of established models. We denote the set of all the feature bases by

$$\mathbf{F}_{\text{all}} = \{\hat{k}_{\text{I}}^{(0)}, \hat{f}_{\text{I}}^{(0)}, \text{sse}_{\text{I}}^{(0)}, \hat{k}_{\text{II}}^{(0)}, \hat{f}_{\text{II}}^{(0)}, \text{sse}_{\text{II}}^{(0)}, \ldots, \hat{k}_{\text{I}}^{(1)}, \hat{f}_{\text{I}}^{(1)}, \text{sse}_{\text{I}}^{(1)}, \ldots, \ldots\}$$

where $\hat{k}_N^{(i)}$, $\hat{f}_N^{(i)}$ are the estimated coefficients of the Nth linear segment of the i-th model in Table I, with $\text{sse}_N^{(i)}$ the standard square error derived from the estimation process.

IV. FAULT DIAGNOSIS

The evaluation of the features is performed by using a hierarchical FPM scheme. This scheme is chosen mostly based on the following considerations:

1) The advantages of a hierarchical tree-like structure are the simple integration of *a priori* knowledge and the intuitive, human-like concept.
2) In a real situation, some faults can be more easily isolated than others. This provides evidence that there must be an intrinsic hierarchical structure in the faults. Therefore, a multiclasses tree-based classifier might be the best choice for our diagnostic system.
3) An FPM method gives a very good classification rate together with a short computing time [9].
4) The defect of the classical FPM method that it cannot be used for discriminating classes of nonconvex shape, has been overcome by two improved classification methods: FPM with exponential function (FPME) and FPM multidensity (FPMM) [11].

A. Construction of HFPMMC

1) Determining the Decision Tree Structure: In this paper, we combine a decision tree structure with FPMM methods to form a multiclasses hierarchical fuzzy matching multidensity classifier (HFPMMC) for the fault diagnosis problem.

To explain the whole tree-building procedure, first some notations should be clarified. We use ALL to denote the root node that stands for the dataset of all training samples.

A set $\mathbf{C}_{\text{all}} = \{C_i | i = 0, 1, \ldots, c-1\}$ is used to denote c classes in ALL. Here, class 0 stands for the successful mating processes and others for the ith fault cases.

The parameter $\mathbf{D}_{\text{all}} = \mathbf{D}_0 \cup \mathbf{D}_1 \cup \cdots \cup \mathbf{D}_{c-1}$ is the set of all training data, where $\mathbf{D}_i$ indicates the training data labeled by C_i.

The parameter $\mathbf{F}_{\text{all}} = \mathbf{F}_0 \cup \mathbf{F}_1 \cup \cdots \cup \mathbf{F}_{c-1}$ is the set of all possible features that are defined in Section III. Here, $\mathbf{F}_i = \{f_i^1, \ldots, f_i^{k_i}\}$ contains all possible features of class C_i. Further, we define $\mathbf{F}_i^* = \{f_i^1, \ldots, f_i^{k_i^*}\} \subseteq \mathbf{F}_i$, which contains k_i^* significant features of class C_i. Note that these significant features are selected model parameters of the class. The detail of the selection method is explained later.

Let m indicate the depth of the decision tree, with $m = 0$, $1, \ldots, c-1$. The parameter $\mathbf{DS}_m \subseteq \mathbf{D}_{\text{all}}$ denotes the dataset dealt with at depth m.

The parameter $\mathbf{C}_m = \{C_{i_{m,1}}, C_{i_{m,2}}, \ldots, C_{i_{m,M_m}}\} \subseteq \mathbf{C}_{\text{all}}$ is used to denote the set of class labels contained in the dataset

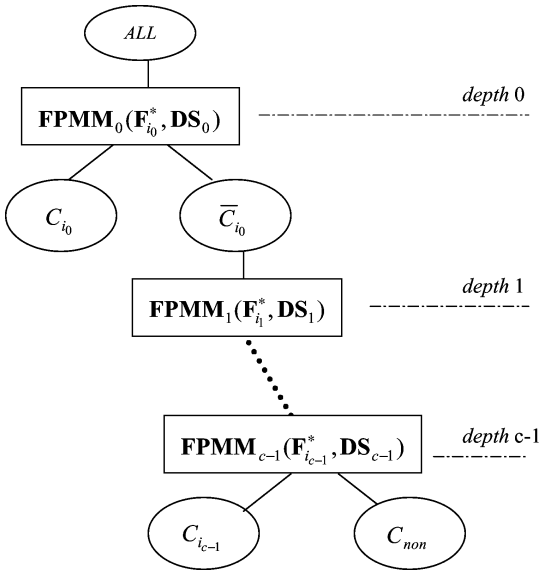

Fig. 8. Hierarchical FPMM classifier.

$\mathbf{DS}_m$, where the integer subscripts satisfy $0 \le i_{m,1} \le \cdots \le i_{m,M_m} \le c-1$. At each depth m, only one class, C_{i_m}, is distinguished from the others within the subspace based on $\mathbf{F}^*_{i_m}$. The variable $\bar{C}_{i_m}$ denotes the other classes in $\mathbf{C}_m$. The subscript i_m satisfies $i_m \in \{i_{m,1}, \ldots, i_{m,M_m}\}$. The variable $C_{\rm non}$ is used to denote all *unknown* data that might appear owing to some unexpected situations.

The parameter $\mathbf{FPMM}_m$ denotes the two-class FPMM classifiers used at depth m.

The expected tree structure of our total classifier is shown in Fig. 8. It should be pointed out that the membership and ambiguity rejects introduced in [11] are applied to classify the "*unknown*" class of data at each depth. Detecting an "*unknown*" sample data is one of the most important abilities of an industrial diagnosis module, since unexpected faults always exist.

2) Choice of Tree Nodes and the Related Feature Subset: In the tree-building procedure, a major problem has to be tackled. That is how to choose the appropriate leaf nodes C_{i_m} and the related feature subset $\mathbf{F}^*_{i_m}$ at depth m.

This task can be divided into two parts. One is to form the feature subset $\mathbf{F}^*_i$ for each class C_i. The other is to decide which class should be isolated at each depth. As mentioned before, elements of the subset $\mathbf{F}_i$ are all model parameters of class C_i, because the developed model reflects the intrinsic properties of this class. In order to obtain $\mathbf{F}^*_i$, feature-selection method has to be applied to reduce the number of features in $\mathbf{F}_i$, which results in both reduced computation and efficient classification. Feature selection is generally performed in two ways. One is to use *a priori* knowledge and experimental observations to choose the most discriminating measurements. The other is to apply some reasonable criteria to search optimal features based on training data. A definition of interclass distance can be used to evaluate how much a feature contributes to the classification performance. The interclass distance of the two-class problem is given by

$$J_j = \frac{(m_{j1} - m_{j2})^2}{s_{j1}^2 - s_{j2}^2} \tag{15}$$

where m_{j1}, m_{j2}, and s_{j1}, s_{j2} are the means and variance of the jth feature of the two classes, respectively.

We form the feature subset $\mathbf{F}^*_i$ by using a method, combining the *a priori* knowledge of force models and the interclass distance criterion. For each class C_i and $\bar{C}_i$, compute the interclass distance J_j over all features of the set $\mathbf{F}_i$. After that, organize the set of interclass distances $\{J_j \mid j = 1, 2, \ldots, k_i\}$ into a descendant order. Finally, evaluate the first n features and select k^*_i of them to constitute $\mathbf{F}^*_i$ in terms of the *a priori* knowledge of modeling. Note that the *a priori* knowledge here means the different significances of the model parameters in a diagnostic task. For instance, phase III of model (12) is found very unstable from experimental observations. Comparing with phase II, it provides less reliable information for diagnosis.

In order to determine the leaf node at depth m, the fuzzy C-mean (FCM) clustering algorithm is applied with each feature subset $\mathbf{F}^*_{i_{m,l}} (l = 1, \ldots, M_m)$, respectively. The cluster validity for the partition is calculated after every clustering under two criteria. One is the *polarization degree* and the other is whether all the samples pertaining to a class belong to the same cluster or not. A similar method can be found in [13].

The complete tree-building procedure using the dataset $\mathbf{D}_{\rm all}$ can then be concluded as follows.

Algorithm 1:

Input: $\mathbf{C}_{\rm all}$, $\mathbf{F}_{\rm all}$, $\mathbf{D}_{\rm all}$.

1) For every class C_i, form the related feature subset $\mathbf{F}^*_i$.
2) Let $m = 0$, $\mathbf{DS}_0 = \mathbf{D}_{\rm all}$, $\mathbf{C}_0 = \mathbf{C}_{\rm all}$,
3) **While** $m < c$ **do**
4) choose the leaf node C_{i_m}.
5) **If** $m < c-1$, **then**
6) learn a 2-classes FPMM classifier by using datasets $\mathbf{D}_{i_m}$, $\mathbf{DS}_m/\mathbf{D}_{i_m}$, and $\mathbf{F}^*_{i_m}$,
7) **Else**
8) employ the dataset $\mathbf{D}_{i_m}$ and $\mathbf{F}^*_{i_m}$ to establish a 2-classes FPMM classifier;
9) **End if**
10) $\mathbf{DS}_{m+1} = \mathbf{DS}_m/\mathbf{D}_{i_m}$, $\mathbf{C}_{m+1} = \mathbf{C}_m/C_{i_m}$, and $m = m+1$;
11) **End while**
12) Output: $\{C_{i_m}, \mathbf{F}^*_{i_m}, \mathbf{FPMM}_m | m = 0, 1, \ldots, c-1\}$.

Because there is no information about the classes other than C_i at depth $c-1$, a threshold Θ is adopted to perform the classification. That is, for a sample x, if the result of fuzzy aggregation computed by $\mathbf{FPMM}_{c-1}$ satisfies $u_i(x) > \Theta$, then x belongs to C_i. Otherwise, it belongs to the *unknown* class $C_{\rm non}$.

B. Fault Diagnosis

The algorithm of fault diagnosis by applying the HFPMMC is specified as follows. Suppose that a new measured sample has been represented as a point x in the feature space based on

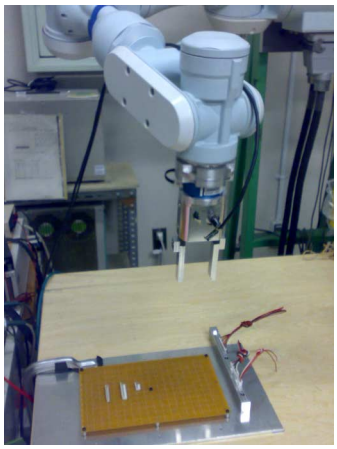

Fig. 9. Experiment setup for a mating process of connectors.

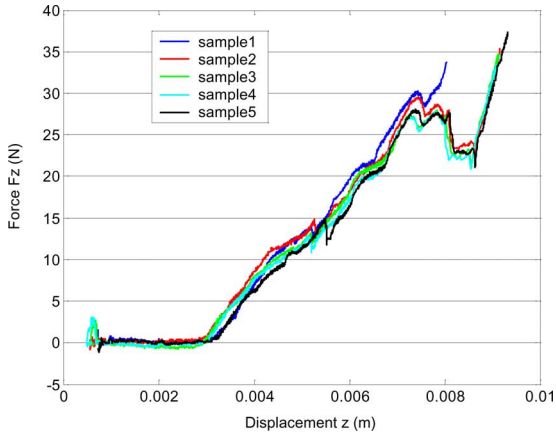

Fig. 10. Several successful mating processes under the same condition.

$\mathbf{F}_{\text{all}}$. $C(x)$ is the final classification result of the hierarchical classifier.

Algorithm 2:

Input: a new point x

1) $m = 0$,
2) **While** $m < c$ **do**
3) use $\mathbf{FPMM}_m$ to classify x based on $\mathbf{F}^*_{i_m}$.
4) **If** x belongs to class C_{i_m} , **then**
5) assign $C(x) = C_{i_m}$ and exit.
6) **End if**
7) $m = m + 1$.
8) **End while,**
9) assign $C(x) = C_{\text{non}}$ and exit.
10) Output: $C(x)$

V. Experiment Results

A. Experimental Condition

A 7 DOF PA-10 industrial robot from MHI was employed to manipulate connectors. Data were acquired from the force sensor and the position sensors mounted in the wrist and joints of PA-10. A base board installed with some headers was fixed in front of the robot. Fig. 9 shows the setup of the experiment.

B. Validation of the Complete Model

The piecewise linear model was validated by a direct comparison of the real experimental data depicted in Figs. 10 and 11. The overall shape of the model is similar to the data, although variations of different connectors and inaccuracies in the modeling procedure make a perfect match impossible. A serious problem in this model is that not only the model parameters are fuzzy, but also the boundary states are unclear. Despite these limitations of the model, it is still useful for fault detection and diagnosis. Typical force profile of fault cases is also shown in Fig. 12.

C. Validation of Parameter Estimation Method

We assessed the accuracy of the identified model by calculating the percentage of the output variation, which is explained by

$$\text{fit} = 1 - \frac{\sum_{k=1}^{n} (F_{z,k} - \hat{F}_z(z_k))^2}{\sum_{k=1}^{n} (F_{z,k} - \bar{F}_z)^2} \tag{16}$$

where $\bar{F}_z$ is the mean value of all the samples $F_{z,k}$. The more this calculated fit is closer to 1, the more accurate this piecewise linear model is.

The results of Table II show that this estimation method is effective for connectors of the same type, even if the mating speed is different.

A comparison of estimated force with actual force data is depicted in Fig. 13.

D. Construction of HFPMMC

The parameter $\mathbf{C}_{\text{all}} = \{C_i | i = 0, 1, \ldots, 4\}$ denotes all the five classes of data in our experiments. The classes include successful mating process and four typical fault cases. According to Table I, the total number of model parameters is 42. Thus, we have a 42-dimensional feature space based on $\mathbf{F}_{\text{all}}$.

To train the HFPMMC, a training dataset $\mathbf{DS}_{\text{all}}$ consisting of 48 samples was employed. There are 16 samples of class C_0 (successful mating) and 8 samples of each of the other classes in $\mathbf{DS}_{\text{all}}$. The reduced feature subset $\mathbf{F}^*_i$ of each class C_i was obtained by applying the feature-selection method presented in Section IV-A2. As mentioned before, the method based on evaluating interclass distances depends severely on the training samples. Bad samples may lead to an unreliable order of features. Thus, *a priori* knowledge and experimental observations are used to choose reliable features that provide interclass distance as long as possible. After determining the classifier's structure, the final HFPMMC was created by Algorithm 1.

E. Validation of HFPMMC

We used a test dataset consisting of 105 samples to validate the classifier. Experimental results show fairly good classification performance. The test dataset were employed to evaluate the final classifier. The success rates of classification for each class were also computed. Table III lists the classification results using trained HFPMMC. All the success ratios are satisfied.

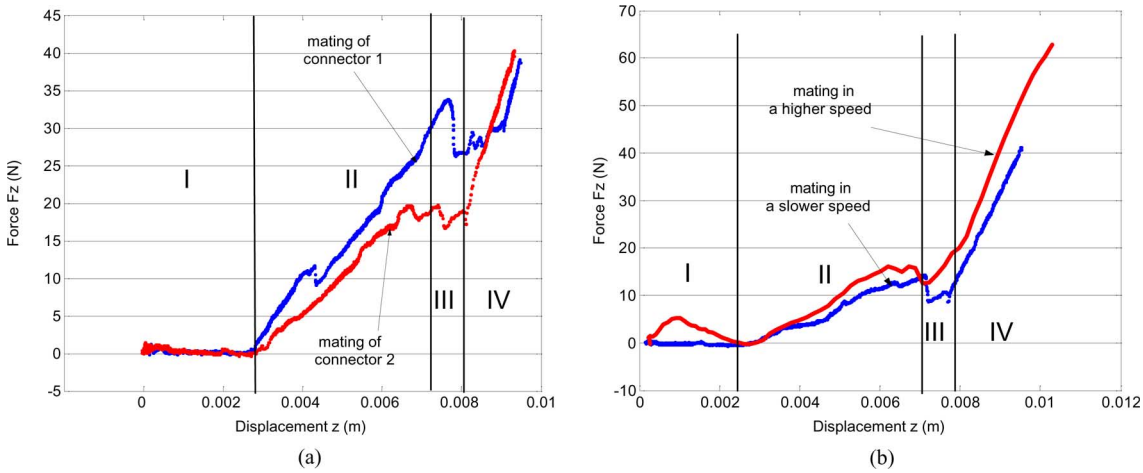

Fig. 11. Force profiles under different experimental conditions. (a) Force profiles of two mating processes using different connectors. (b) Force profiles of two mating processes with different mating speeds.

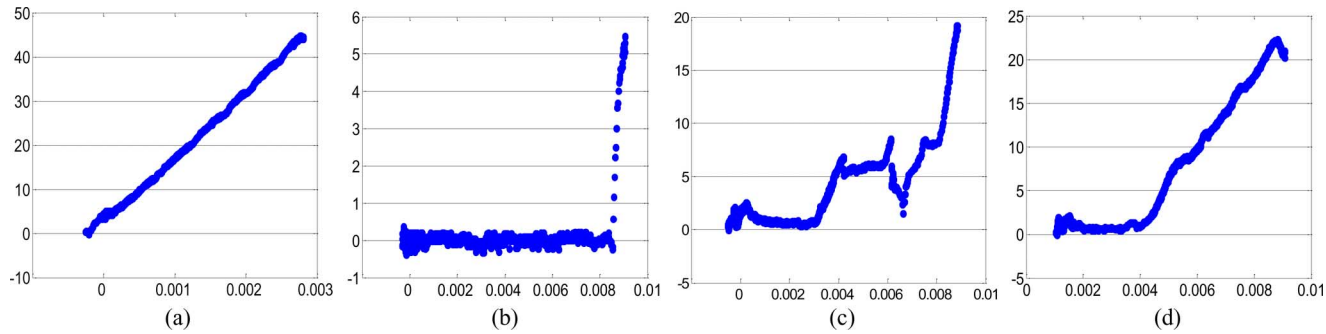

Fig. 12. Typical force profiles of fault cases. (a) Fault I. (b) Fault II. (c) Fault III. (d) Fault IV.

TABLE II
VALIDATION OF THE PARAMETER ESTIMATION

connectors	*fit*	
	Mating in a lower speed	***Mating in a higher speed***
1	0.9749	0.9228
2	0.9445	0.8848

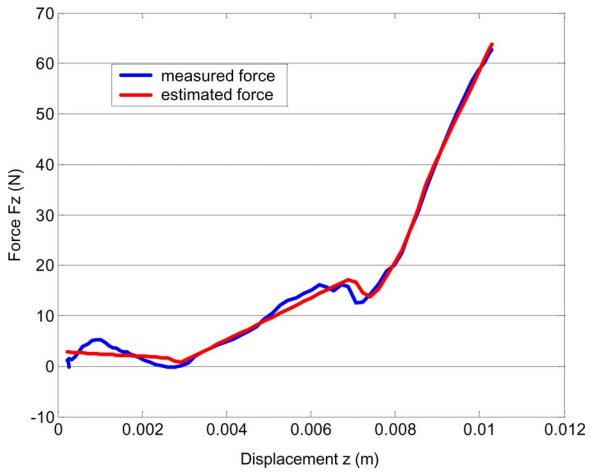

Fig. 13. Comparison of measured force data and estimated one.

TABLE III
RESULTS USING TRAINED HFPMMC

Class	Test dataset			
	Number of correctly classified data	Number of wrongly classified data	Number of unknown data	Success rate of classification
0	53	1	1	96.4%
1	19	1	0	95.0%
2	15	0	0	100%
3	4	1	0	80.0%
4	8	2	0	80.0%

VI. CONCLUSION

In this paper, we proposed a kind of static piecewise linear model to describe the successful robotic mating process of electric connectors, as well as several possible fault cases. The experimental results show that this modeling methodology has good accuracy for identifying such processes. Although only one typical connector was investigated, the method can be extended to other types of connectors easily. To realize a practical fault detection and diagnostic system, a new multiclasses classifier called the HFPMMC was also proposed. The classifier provides good performance in fault diagnosis. The effectiveness of the proposed methods is confirmed by experiments.

As a future work, we intend to study the error recovery system for the mating process, where a new real-time fault detection and diagnosis scheme is required. To further enhance the performance of fault diagnosis, other sensors like vision systems would be added into the system.

ACKNOWLEDGMENT

The authors would like to thank reviewers for their constructive comments.

REFERENCES

[1] D. Henrich and H. Wörn, *Robot Manipulation of Deformable Objects*. (Advanced Manufacturing Series). London, U.K.: Springer-Verlag, 2000, pp. 92–134.
[2] T. Matsuno, D. Tamaki, F. Arai, and T. Fukuda, "Manipulation of deformable linear objects using knot invariants to classify the object condition based on image sensor information," *IEEE Trans. Mechatronics*, vol. 11, no. 4, pp. 401–408, Aug. 2006.
[3] P. Loborg, "Error recovery in automation: An overview," in *Proc. AAAI 1994 Spring Symp. Detecting Resolving Errors Manuf. Syst.*, Stanford, CA, pp. 94–100.
[4] T. Sorsa and H. Koivo, "Application of artificial neural networks in process fault diagnosis," *Automatica*, vol. 29, no. 4, pp. 843–849, Jul. 1993.
[5] C. Frey and H. Kuntze, "A neuro-fuzzy supervisory control system for industrial batch processes," *IEEE Trans. Fuzzy Syst.*, vol. 9, no. 4, pp. 570–577, Aug. 2001.
[6] R. Isermann, "Special section on supervision, fault detection and diagnosis of technical systems," *Control Eng. Pract.*, vol. 5, no. 5, pp. 637–719, May 1997.
[7] R. Isermann, "Model-based fault detection and diagnosis—Status and applications," in *Proc. 16th Symp. Autom. Control Aerosp.*, St. Petersburg, Russland, 2004, pp. 14–18.
[8] P. Ballé and D. Fuessel, "Closed-loop fault diagnosis based on a nonlinear process model and automatic fuzzy rule generation," *Eng. Appl. Artif. Intell.*, vol. 13, no. 6, pp. 695–704, Dec. 2000.
[9] P. Billaudel, A. Devillez, and G. V. Lecolier, "Performance evaluation of fuzzy classification methods designed for real time application," *Int. J. Approx. Reason.*, vol. 20, no. 1, pp. 1–20, Jan. 1999.
[10] M. S. Mouchaweh, A. Devillez, G. V. Lecolier, and P. Billaudel, "Incremental learning in fuzzy pattern matching," *Fuzzy Sets Syst.*, vol. 132, no. 1, pp. 49–62, Nov. 2002.
[11] A. Devillez, "Four fuzzy supervised classification methods for discriminating classes of non-convex shape," *Fuzzy Sets Syst.*, vol. 141, no. 2, pp. 219–240, Jan. 2004.
[12] D. Fuessel and R. Isermann, "Hierarchical motor diagnosis utilizing structural knowledge and a self-learning neuro-fuzzy scheme," *IEEE Trans. Ind. Electron.*, vol. 47, no. 5, pp. 1070–1077, Oct. 2000.
[13] S. W. Jung, S.-W. Bae, and G.-T. Park, "A design scheme for a hierarchical fuzzy pattern matching classifier and its application to the tire tread pattern recognition," *Fuzzy Sets Syst.*, vol. 65, no. 2/3, pp. 311–322, 1994.
[14] S. Schaal and C. Atkeson, "Constructive incremental learning from only local information," *Neural Comput.*, vol. 10, no. 8, pp. 2047–2084, Nov. 1998.
[15] L. Kiong, M. Rajeswari, and M. Rao, "Extrapolation detection and novelty-based node insertion for sequential growing multi-experts network," *Appl. Soft Comput.*, vol. 3, no. 2, pp. 159–175, Sep. 2003.

Jian Huang (M'08) received the B.S. degree in automatic control engineering in 1997, and the M.S. and Ph.D. degrees in control theory and control engineering from Huazhong University of Science and Technology (HUST), Hubei, China, in 2000 and 2005, respectively.

He is currently a Postdoctoral Researcher in the Department of Micro-Nano System Engineering and the Department of Mechano-Informatics and Systems, Nagoya University, Nagoya, Japan. He is also a Lecturer in the Department of Control Science and Engineering, HUST. His current research interests include robotic assembly, networked control systems, and bioinformatics.

Toshio Fukuda (M'83–SM'93–F'95) received the B.S. degree from Waseda University, Tokyo, Japan, in 1971, the M.S. degree in 1973, and the Ph.D. degree with a dissertation entitled "Malfunction diagnosis and application of stable adaptive schemes for a nuclear reactor system," in 1977, both from the University of Tokyo, Tokyo, Japan.

From 1977 to 1982, he was with the National Mechanical Engineering Laboratory, Tsukuba, Japan. From 1982 to 1989, he was with the Science University of Tokyo. Since 1989, he has been with Nagoya University, Nagoya, Japan, where he is currently a Professor in the Department of Micro-Nano Systems Engineering. His current research interests include intelligent robotic systems, cellular robotic systems, mechatronics, and micro-nanorobotics.

Dr. Fukuda was the President of the IEEE Robotics and Automation Society (1998–1999), the Director of the IEEE Division X, Systems and Control (2001–2001), and the Editor-in-Chief of the IEEE/AMERICAN SOCIETY OF MECHANICAL ENGINEERS TRANSACTIONS ON MECHATRONICS (2000–2002), and the President of the IEEE Nanotechnology Council (2002–2005). He is the AdCom President of the IEEE Nanotechnology Council.

Takayuki Matsuno (M'05) received the B.S., M.S., and Ph.D. degrees in micro system engineering from Nagoya University, Nagoya, Japan, in 1998, 2000, and 2005, respectively.

He was a Research Associate in the Department of Micro-Nano System Engineering and the Department of Mechano-Informatics and Systems, Nagoya University, untill March 2006. He is currently a Research Associate in intelligent systems design engineering, Toyama Prefectural University, Imizu City, Japan. His current research interests include flexible object manipulation, automation of assembly task in factories, and dynamical system control.